Sub-wavelength patterning of the optical near-field

Romain Quidant[1], **Gonçal Badenes**[1], **Stéphanie Cheylan**[1], **Ramon Alcubilla**[2], **Jean-Claude Weeber**[3], **Christian Girard**[4]

[1] *ICFO–Institut de Ciències Fotòniques, Jordi Girona 29, Nexus II, 08034 Barcelona, Spain*
[2] *Universitat Politècnica de Catalunya, C-4 Campus Nord, Gran Capitan s/n, 08034 Barcelona, Spain*
[3] *LPUB, UMR-CNRS 5027, 9 av. A. Savary, 21078 Dijon, France*
[4] *CEMES, UPR-CNRS 8011, 29 rue Jeanne Marvig, 31055 Toulouse, France*

Romain.Quidant@upc.es

http://www.icfo.es

Abstract: We report the sub-wavelength patterning of the optical near-field by total internal reflection illumination of a regular array of resonant gold nano-particles. Under appropriate conditions, the in-plane coupling between Localized Surface Plasmon (LSP) fields gives rise to sub-wavelength light spots between the structures. Measurements performed with an Apertureless Scanning Near-Field Optical Microscope (ASNOM) show a good agreement with theoretical predictions based on the Green dyadic method. This concept might offer a convenient way to elaborate extended optical trap landscapes for manipulation of sub-micrometer systems.

OCIS codes: (180.5810) Scanning Microscopy; (240.5420) Polaritons; (260.3910) Metals optics of; (350.3950) Micro-optics

References and links

1. J. M. Vigoureux and D. Courjon, “Detection of non radiative fields in light of the Heisenberg uncertainty principle and the Rayleigh criterion”, Appl. Opt. **31**, 3170 (1992)
2. J. T. Takahara, S. Yamagishi, H. Taki, A. Morimoto, and T. Kobayashi, “Guiding of a one-dimensional optical beam with nanometer diameter,” Opt. Lett. **22**, 475 (1997)
3. H. A. Bethe, “Theory of Diffraction by Small Holes,” Phys. Rev. **66**, 163 (1944)
4. T. W. Ebbesen, H. J. Lezec, H. F. Ghaemi, T. Thio, and P. A. Wolff, “Extraordinary optical transmission through sub-wavelength hole arrays,” Nature (London) **391**, 667 (1998)
5. H. J. Lezec, A. Degiron, E. Devaux, R. A. Linke, L. Martin-Moreno, F. J. Garcia-Vidal, and T. W. Ebbesen, “Beaming light from a Subwavelength Aperture,” Science **297** (2002)
6. C. Chicanne, T. David, R. Quidant, J. C. Weeber, Y. Lacroute, E. Bourillot, A. Dereux, G. Colas-des-Francs, and C. Girard, “Imaging the Local Density of States of Optical Corrals,” Phys. Rev. Lett. **88**, 097402 (2002)
7. C. Bohren and D. Huffman, *Absorption and scattering of light by small particles* (John Wiley, New-York, 1983).
8. M. Meier, A. Wokaum, and P. F. Liao, “Enhanced fields on rough surfaces: dipolar interaction among particles of sizes exceeding the Rayleigh limit,” J. Opt. Soc. Am. B **2**, 931 (1985).
9. B. Lamprecht, G. Schider, R. T. Lechner, H. Ditbacher, J. R. Krenn, A. Leitner, and F. R. Aussenegg, “Metal Nanoparticle Gratings: Influence of Dipolar Particle on the Plasmon Resonance,” Phys. Rev. Lett. **84**, 4721 (2000).
10. N. Felidj, J. Aubard, G. Lévi, J. R. Krenn, M. Salermo, G. Schider, B. Lamprecht, A. Leitner, and F. R. Aussenegg, “Controlling the optical response of regular arrays of gold particles for surface-enhanced Raman scattering,” Phys. Rev. B **65**, 075419 (2002)
11. L. Gunnarsson, E. J. Bjerneld, H. Xu, S. Petronis, B. Kasemo, and M. Käll, “Interparticles coupling effects in nanofabricated substrates for surface-enhanced Raman scattering,” Appl. Phys. Lett. **78**, 802 (2001)
12. O. J. F. Martin, C. Girard, and A. Dereux, “Generalized Field Propagator for Electromagnetic Scattering and Light Confinement,” Phys. Rev. Lett. **74**, 526 (1995).

#3515 - $15.00 US Received 12 December 2003; revised 9 January 2004; accepted 12 January 2004

13. J.-J. Greffet and R. Carminati, “Image formation in near-field optics,” Progress in Surface Science **56**, 133 (1997).
14. C. Girard, A. Dereux, O. J. F. Martin, M. Devel, “Generation of optical standing waves around mesoscopic surface structure: scattering and light confinement,” Phys. Rev. B **52**, 2889 (1995)
15. H. Melville, G. F. Milne, G. C. Spalding, W. Sibbett, K. Dholakia, and D. McGloin, “Optical trapping of three-dimensional structures using dynamic holograms,” Opt. Express **11**, 3562 (2003) http://www.opticsexpress.org/abstract.cfm?URI=OPEX-11-26-3562
16. M. P. MacDonald, G. C. Spalding, and K. Dholakia, “Microfluidic sorting in an optical lattice,” Nature (London) **426**, 421 (2003)
17. Y. Inouye and S. Kawata, “Near-field scanning optical microscope with a metallic probe tip,” Opt. Lett. **19**, 159 (1994)
18. F. Zenhausern, M. P. O’Boyle, and H. K. Wickramasinghe, “Apertureless near-field optical microscope,” Appl. Phys. Lett. **65**, 1623 (1994)
19. R. Bachelot, P. Gleyzes, and A. C. Boccara, “Near-field optical microscope based on local perturbation of a diffraction spot,” Opt. Lett. **20**, 1924 (1995)
20. R. Hillenbrand and K. Keilmann, “Complex Optical Constants on a Subwavelength Scale,” Phys. Rev. Lett. **85**, 3029 (2000)
21. A. Madrazo, R. Carminati, M. Nieto-Vesperinas, and J. J. Greffet, “Polarization effects in the optical interaction between a nanoparticle and a corrugated surface: implications for apertureless near-field microscopy,” J. Opt. Soc. Am. A **15**, 109 (1998)
22. S. Blaize, S. Aubert, A. Bruyant, R. Bachelot, G. Lerondel, P. Royer, J. E. Broquin, and V. Minier, “Apertureless scanning near-field optical microscopy for ion exchange waveguide characterization,” Journal of Microscopy **209**, 155 (2002).
23. J. A. Porto, P. Johansson, S. P. Apell, and T. López-Ríos, “Resonance shift effects in apertureless scanning near-field optical microscopy,” Phys. Rev. B **67**, 085409 (2003)
24. A. Pack, W. Grill, and R. Wannemacher, “Apertureless near-field optical microscopy of metallic nanoparticles,” Ultramicroscopy **94**, 109 (2003)
25. R. Fikri, T. Grosges, and D. Barchiesi, “Apertureless scanning near-field optical microscopy: the need for probe-vibration modeling,” Opt. Lett. **28**, 2147 (2003)
26. S. Kawata and T. Sugiura, “Movement of micrometer-sized particles in the evanescent field of a laser beam,” Opt. Lett. **17**, 772 (1992)
27. K. Okamoto and S. Kawata, “Radiation Force Exerted on Subwavelength Particles near a Nanoaperture,” Phys. Rev. Lett. **83**, 4534 (1999)

In the ongoing general trend for miniaturization, optics has shown much more difficulty than electronics to reach the nanometric regime. A main reason for this delay is the physical limit imposed by diffraction when focusing light. Indeed, the smallest diameter of an optical beam propagating in a dielectric medium of refraction index n is of the order of $\lambda = \lambda_0/n$, λ_0 being the wavelength in free space. This condition can be derived easily from one dimensional Fourier analysis:

$$\Delta x \Delta k_x \geq 2\pi$$

where Δx and Δk_x are, respectively, the spatial extension of the beam in the x axis and the Fourier spectrum of the corresponding wave-vector. When, in free space, Δx is reduced below $\lambda/2$, k_x reaches values greater than ω/c and the associated wave becomes non-propagative [1]. Reciprocally, confining light from a 3D laser beam (with its three k vector components real) down to sub-wavelength (sub-λ) sizes imposes a reduction on its dimensionality [2].

The possibility of controlling the confinement of light within sub-λ volumes is of great interest in various fields of application ranging from high density data storage to optical circuitry and also for sensing and optical trapping. In the case of optical trapping, research in biology and medicine would highly benefit from the miniaturization of optical traps down to the nanometer scale, allowing the direct and non-destructive manipulation of very small living entities. In this paper we investigate a surface structure that can locally enhance optical potential gradients. Such potential gradients, through the multipolar-gradient interactions, might offer the opportunity of optically confining nanosystems close to surfaces in relatively deep traps and controlling their transport through them.

To achieve a non-diffraction limited light confinement, it was recently suggested to use a

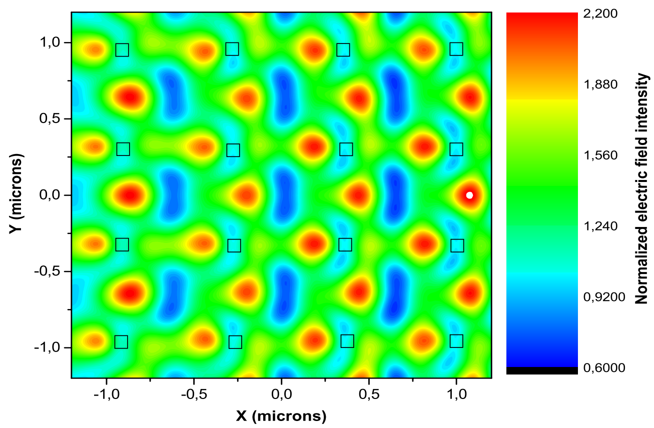

Fig. 1. Theoretical map of the near-field electric intensity calculated 100 nm above a 5×6 array (640 nm period) of gold pads $(100\times100\times40)\,\text{nm}^3$ (location represented by the black squares). The illumination is performed by a plane wave (633 nm, TM polarization) under total internal reflection (45° incidence angle). The normalization at each point is done with respect to the electric intensity in the observation plane in the absence of any nanostructure.

surface patterned with nano-structures. A first possible way consists of using the transmission through a sub-λ aperture designed in a metallic film [3, 4]. Latest works have demonstrated that the properties of the emerging light can be modified by appropriately patterning the vicinity of the hole [5]. The method we propose uses arrays of nano-particles lying on top of a dielectric surface. Under appropriate conditions, the in-plane interferences between the fields scattered by the nanostructures can generate a field landscape with sub-λ features. This can be also described in terms of the modification of the electromagnetic local density of states at the interface by the nano-particles [6]. In order to optimize this effect, the scattering power from each individual nano-center constituting the ensemble should be maximized. For this reason we have chosen to work with gold metal nano-particles sustaining Localized Surface Plasmons (LSPs). LSPs are resonant electromagnetic eigenmodes which give rise to spectrally selective light absorption and scattering, and to a considerable enhancement of the local electromagnetic fields [7]. The LSP frequency depends mainly on particle geometry and on the dielectric constants of both the constitutive metal and the surrounding medium. Recently, collective effects within periodic ensembles of resonant nanoparticles have been intensively studied [8, 9]. On this basis, optimized regularly patterned surfaces are proposed as efficient substrates for Surface Enhanced Raman Scattering (SERS) analysis [10, 11].

In order to find the optimum structural and illumination parameters for generating tiny light spots at a decorated surface, we have performed extensive numerical simulations based on the Green dyadic method [12, 13]. Such *ab initio* investigation of the optical near-field distributions only requires a specification of the frequency-dependent dielectric constant and the precise shape of the structures. The distribution of the electric near-field map was calculated above various finite gratings of gold nano-pads lying onto a glass substrate when illuminated by a plane wave under total internal reflection. Figure 1 shows the electric near-field intensity map calculated 100 nm above a 5 by 6 matrix with period 640 nm, where each pad is a parallelepiped with a 100 nm side square basis and 40 nm height. The illumination was performed at $\lambda = 633\,\text{nm}$

#3515 - $15.00 US Received 12 December 2003; revised 9 January 2004; accepted 12 January 2004

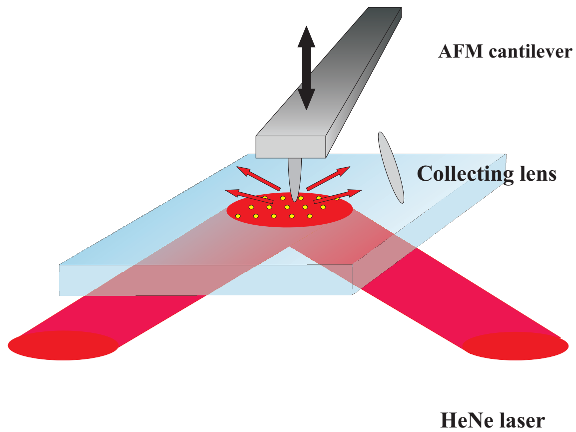

Fig. 2. Schematic description of our ASNOM set-up

where the particles are resonant. The incident field polarization state was TM (Transverse Magnetic) and the reflection angle was 45°. One can first notice at the left hand of each nano-pad a high-intensity spot associated with its LSP mode. The coherent summation of the LSP fields gives rise to additional sub-λ features between the structures. Especially, a minimum and a maximum of intensity appear within the square unit cell. The maxima have an average diameter of 150 nm (FWHM) corresponding to less than one fourth of the incident wavelength. Note that the absence of symmetry observed with regard to the axis $X = 0$ finds its origin both in the asymmetry of the illumination and (mainly) in the finite size of the simulated grating, which was limited by the available computer memory. In the calculation plane considered, which is located 100 nm above the surface, the electric field intensity contrast is $I_{max}/I_{min} \simeq 4$. Due to the exponential decay nature of evanescent fields, the contrast strongly increases as the surface is approached [14]. The resulting sharp 3D field gradients provide a well-contrasted optical potential landscape suitable for the manipulation of dielectric nano-systems. While the transversal gradient of the near-field assures the confinement at the surface vicinity, the in-plane modulation offers localized sites that might be used for simultaneous multiple trapping [15] and sorting [16].

On the basis of the numerical results, a sample was fabricated by standard electron beam lithography using a JEOL 6500 scanning electron microscope (SEM) equipped with a lithography system from RAITH. The e-beam patterning was first performed on a single layer of polymethylmethacrylate (PMMA) resist (950 K molecular weight and 120 nm thickness). After development of the PMMA film, 40 nm of gold were thermally evaporated before dissolving the remaining resist. The resulting sample consists of several 200 μm × 200 μm periodic arrays of gold nano-particles. The particles are half oblate spheroids with typical dimensions 100 nm diameter section and 40 nm height. The period is 650 ± 20 nm. Extinction measurements performed with unpolarized white light on each ensemble give a LSP resonance centered around 650 nm and extended over about 80 nm (FWHM). Figure 3(a) shows a 2.4 μm × 2.4 μm Atomic Force Microscope (AFM) image recorded on one of the matrixes.

Measuring the distribution of the electromagnetic field above the decorated surface requires the sensitivity to evanescent fields of optical near-field microscopy. In this study, we have chosen to work with the ASNOM configuration where the probe is a conventional AFM tip coated with an appropriate metal layer [17, 18, 19, 20]. The main advantages of this configuration compared to other ones using a sharply elongated optical fiber are the tip robustness and reproducibility. Our setup was developed on a commercial AFM D3100 (Digital Instruments)

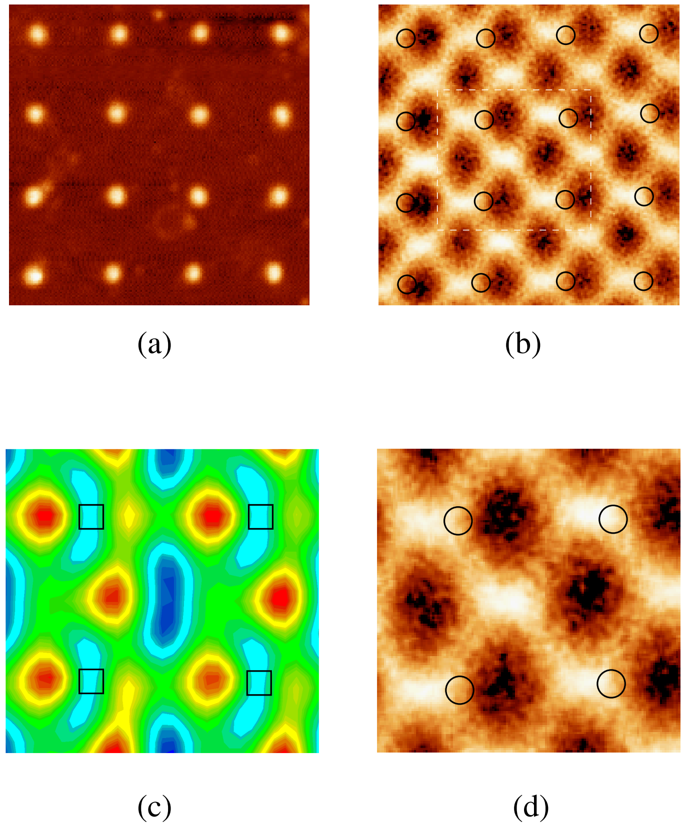

Fig. 3. (a-b) $2.4\,\mu m \times 2.4\,\mu m$ images recorded simultaneously above the fabricated sample. (a) AFM topography, (b) ASNOM image ($\lambda = 632.8\,nm$, TM polarization and 45° incidence angle). (c-d) Comparison over a unit cell of the theoretical near-field electric intensity (c) and the experimental measurements (d) (zoom in on the square area drawn on Fig. 3(b)).

where the sample chuck was replaced by a custom-made stage allowing both the sample illumination from an external laser and the detection of the near-field information. As sketched in Fig. 2, the sample lying on top of a glass prism is illuminated under total internal reflection by a collimated beam (beam waist $400\,\mu$m) from a HeNe laser ($\lambda_0 = 632.8\,$nm, $15\,$mW). The fields scattered by the Pt coated silicon tip when scanning the sample surface in tapping mode (oscillation amplitude of about 50 nm at a frequency of 280 kHz) are collected on the side by a lens (NA $= 0.15$, working distance $= 15\,$mm) and sent towards a highly sensitive photomultiplier tube (Hamamatsu R943-02). In order to extract the near-field information, the collected signal is demodulated at the oscillation frequency of the cantilever. Under this operation mode the signal measured by an ASNOM is known to be proportional to the electric field intensity below the scanned tip [21, 22].

Figure 3(b) shows a typical ASNOM measurement recorded on the fabricated sample when the illumination conditions closely match the ones used in the simulation shown in Fig. 1. The optical map clearly displays a periodic pattern of bright and dark spots. The actual position of the particles can be precisely located within the field landscape using the AFM topographical image that was simultaneously recorded. This makes it possible to perform a direct comparison with the theoretical near-field electric intensity map. As predicted by the simulation, clearly

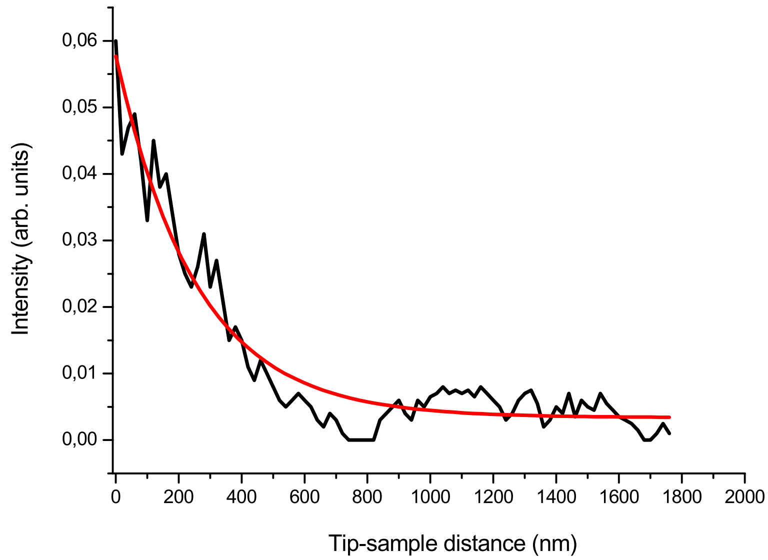

Fig. 4. Dependence of the ASNOM signal on the tip-sample distance when precisely located above one of the inter-particle maxima (experimental data in black, fitting in red).

localized intensity maxima appear between the particles. They display an elliptic shape with 150 nm short axis and 250 nm long axis. In order to evaluate their extension in the third dimension, normal to the sample surface, we measured the dependence of the ASNOM signal on the tip-surface distance when the probe is precisely located above one of the maxima positions (Fig. 4). The exponential decay confirms the evanescent nature of the associated fields and gives a transversal confinement at $1/e^2$ of about 500 nm.

While the ASNOM image reproduces the main features of the theoretical near-field electric intensity distribution above the sample, significant differences can be observed, especially in terms of the position and magnitude of the dark spots (Figs. 3(c-d)). These differences may result partially from the geometric deviation of the particles with respect to the ideal pads considered in the simulation. Nevertheless, we attribute them mainly to the acquisition process. Indeed, the high dielectric constant of the probe may create a significant perturbation of the intrinsic electromagnetic properties of the sample when precisely located above the particles [23, 24]. Furthermore, very recent work demonstrates that a full prediction of ASNOM measurements requires taking into consideration the tip modulation [25].

To conclude, we have shown in this study how a glass surface patterned with a regular array of gold nano-structures can generate a regular field landscape with sub-λ features. ASNOM measurements performed on a nanofabricated sample were found to be in good qualitative agreement with the predicted near-field electric intensity map even if the influence of the detection procedure remains to be further investigated. The resulting periodic array of subwavelength inter-particle spots, featuring a sharp field gradient in the three dimensions, may constitute an optical potential landscape for manipulating sub-micrometer systems [26, 27].

Acknowledgments

This research has been supported by the Generalitat de Catalunya. Support by the European Union, through the European Regional Development Fund, is also acknowledged.

 Received 12 December 2003; revised 9 January 2004; accepted 12 January 2004
